Hindawi
Advances in Civil Engineering
Volume 2019, Article ID 6805480, 7 pages
https://doi.org/10.1155/2019/6805480

Research Article

Research on the Mechanical Properties and NMR Characteristics of Cement Mortar during Freeze-Thaw Cycles

Taoying Liu,[1,2,3] **Yunmin Wang**,[1,3] **Keping Zhou**,[2,3] **Feng Gao**,[1,2,3] **and Shenghua Xie**[1,3]

[1]*Sinosteel Maanshan Institute of Mining Research Co., Ltd., Ma'anshan, Anhui 243004, China*
[2]*School of Resources & Safety Engineering, Central South University, Changsha, Hunan 410083, China*
[3]*The State Key Laboratory of Safety and Health for Metal Mine, Ma'anshan, Anhui 243004, China*

Correspondence should be addressed to Taoying Liu; taoying_liu@163.com

Received 4 May 2018; Revised 31 July 2018; Accepted 23 December 2018; Published 27 February 2019

Academic Editor: Dong-Sheng Jeng

Low-field nuclear magnetic resonance (NMR) technology has the characteristics of nondestructive, rapid, and accurate. In the present paper, the mechanical properties and the size and distribution of pores of cement mortar during freeze-thaw cycles were studied by using the NMR technology for the first time. The change law of surface and quality, compressive strength, splitting tensile strength, and elastic modulus of cement mortar under 0, 25, 50, 75, and 100 freeze-thaw cycles were studied. And the changes of T_2 spectra of cement mortar under different freeze-thaw environments were analyzed; the change rule between freeze-thaw cycles and the size of the pore within the cement mortar were also obtained. Moreover, the relationship between the mechanical properties and the pore structure of cement mortar was studied.

1. Introduction

In recent years, there are more and more concrete engineering developed in the cold regions [1, 2], and the need to accurately evaluate the stability of geotechnical engineering constructions and to prevent or control freeze-thaw hazards has become an urgent problem [3, 4]. Studies of the physical and mechanical properties of building material that undergo freeze-thaw cycles provide important data for the prevention of freeze-thaw hazards in cold regions. Low concrete temperature reduces the rate of the strength gain and extends the setting time [5, 6]. Freezing and thawing cycles deteriorate concrete because water freezes to ice and expands, and the volume change of water to ice causes high stress if there is no room for expansion. The ice then melts down water and increases the saturation level of the voids [7, 8]. Powers [9] originally proposed that hydraulic pressure (as water freezes, it expands and generates pressure on the pore wall) was the source of stress that causes damage. The following cycles of freezing and thawing in cold climates aggravate the resistance of the concrete [10, 11]. The increase of the volume of a fluid phase at freezing results in the occurrence of some effects: the crystallizing pressure of ice upon the walls of the pores and capillaries, the hydraulic pressure of the porous liquid, and the osmotic pressure caused by the freezing of water [12, 13]. Concrete internal damage caused by the frosting of internal moisture within concrete pores will lead to the generation and disintegration of microcracks. Studies of the pore structure of properties of cement mortar that undergo freeze-thaw cycles will provide important data for analyses of cement mortar engineering and the prevention of freeze-thaw hazards in cold regions.

Current detections of microscopic deterioration of solid materials are mainly conducted with traditional methods like the technique of CT scanning [14, 15], method of scanning electron microscope (SEM) [16], technique of digital imaging treatment [17], and acoustic emission [18, 19], yet these methods are not very satisfying. For example, results of CT scanning cannot reflect the features of microscopic structure [20, 21], and the experiment is costly; the method of electron microscope requires small specimen, and it can only be used in real time observation. As a new method for analysis and detection in physical tests, nuclear magnetic resonance (NMR) technology has the characteristics of nondestructive, rapid, and accurate [22], and it can be used to obtain parameters such as porosity, free fluid

index, pore-size distribution, and T_2 distribution of transverse relaxation time [23, 24]. It could be applied in experiments and detection researches on pore-size distribution, characteristics of the inner structure of concrete, and so on [25, 26]. In the present study, an extensive testing program is conducted to investigate the effect of concrete after freeze-thaw attack. The NMR technique was also applied to the measurement of concrete specimens. The mechanical property test is performed on the specimens after different freeze-thaw cycles. Freeze-thaw effects on the surface scaling, weight loss, water content, compressive strength, and elastic modulus are discussed and clarified. Several conclusions are then drawn based on the proposed study.

2. Experimental Methods

2.1. NMR Technology. Nuclear magnetic resonance (NMR) refers to the response of atomic nuclei to magnetic fields. Many nuclei have a magnetic moment, and they behave like a spinning bar magnet. These spinning magnetic nuclei can interact with externally applied magnetic fields, producing a measurable signal. The hydrogen proton (H+) is a particle with a positive charge, and proton spin is one of the important properties of the hydrogen proton. Hydrogen proton spin can produce a magnetic field, and magnetic axis directions of protons are random in no external magnetic field. The porosity of saturated cement mortar can be calculated by substituting the amplitudes of the detected signals into the relation determined by calibration samples. The porosity indicates the water content and volume in the cement mortar. If the specimens tested by the NMR are water saturated, the water volume is equal to the crack volume.

T_2 is a time constant describing decay of the transverse component of magnetization. According to nuclear magnetic resonance theory, the transverse relaxation rate of nuclear magnetic resonance can be expressed as the following equation [24]:

$$\frac{1}{T_2} = \frac{1}{T_2^1} + \frac{\rho_2 s}{V} + \frac{D(\gamma G T_E)^2}{12}, \quad (1)$$

where T_2^1 is the relaxation time of fluid, ρ_2 is the transverse surface relaxation strength, s is the pore surface area, V is the pore volume, $(\rho_2 s)/V$ is the transverse surface relaxation rate, D is the diffusion coefficient, γ is the gyromagnetic ratio, G is the gradient of the magnetic field, T_E is the echo time, and $(D(\gamma G T_E)^2)/12$ is the diffusion relaxation rate.

In this study, there is only one type of fluid (water) in the pores, and the volume relaxation is much slower than that of the area, so $1/T_2^1$ is neglected. When the magnetic field is even and T_E adopted is short, the diffusion relaxation can also be ignored. Therefore, equation (1) can be simplified as

$$\frac{1}{T_2} = \frac{1}{T_2^1} + \frac{\rho_2 s}{V}. \quad (2)$$

From equation (2), the rate of transverse relaxation depends on the surface-to-volume ratio of the pores. Thus, the T_2 distribution reflects the pore size information: the smaller the T_2 value is, the smaller the pore size is; the larger the T_2 value is, the larger the pore size is.

2.2. Experimental Scheme. The cement mortar specimens were made of a mixture of water and cement according to the standard GB/T50082-2009. Ordinary Portland cement 42.5 R was used in this experiment, and the test report is shown in Table 1. The river sand is collected from the Xiangjiang river; the apparent density is 2640 kg/m^3, bulk density is 1430 kg/m^3, silt content is 0.8%, and fineness modulus is 2.91. The cement mortar mixture scheme is shown in Table 2.

The main experimental equipment included freeze-thaw cycle test machine, vacuum saturation device, NMR test system, and loading control system DCS-200, as shown in Figure 1. The NMR measurements were conducted using an AniMR-150 NMR system. The NMR test system was supplied by Niumag Corporation (Shanghai, China) with wide bore and vertical superconducting magnet. The magnetic field strength reaches 0.25 T, and the resonance frequency ranges from 8.5 to 12.8 MHz. The gradient coils can provide a maximum gradient strength of 0.15 T/m in X, Y, and Z directions, respectively. The required temperature of the experimental environment is 32°C to guarantee the system. Experimenting at such a temperature also ensures the testing system run at its best. The porosity, T_2 distribution, and MR image can be obtained by using the Core analysis software and the MRI viewer software.

The main steps of the test are as follows. (1) After casting molding and 24 hours of conservation, the cement mortar was placed in the standard curing box under the curing condition 20 ± 3°C and 95% RH. (2) The specimens were tested according to the standard experimental procedure. (3) The specimens were saturated by vacuum saturation device for 12 h and then placed in the freeze-thaw cycle test machine under the condition of freezing temperature of −20°C and thawing temperature of 20°C with reference to the weather condition. Each complete cycle of freeze-thaw lasted for 8 h, comprising 4 h for freezing and 4 h for thawing. (4) The specimens from the freeze-thaw cycle test machine were removed, water on the surface was wiped off, and the variations of appearance were recorded. (5) Porosity and T_2 distribution were obtained by the NMR technology. (6) After recording the change rule of quality during NMR experiment, the next freeze-thaw test are carried out. The dimension of the additive cement mortar specimens was 70.7 mm × 70.7 mm × 70.7 mm, as shown in Figure 2.

3. Cement Mortar Damage Evolution during Freeze-Thaw Cycle

By observing the surface changes of the cement specimens during the freeze-thaw cycles as shown in Figure 3, there was no obvious change on the cement mortar after 75 cycles, but it had changed significantly after 100th cycles. There was a weak side on the surface that damaged after many freeze-thaw cycles, while the lower layer did not change much.

Table 1: P.O 42.5 R Portland cement quality performance metrics.

Initial setting times	Final setting time	Compressive strength (MPa)		Breaking strength (MPa)		Fineness (%)	Loss on ignition (%)	MgO content (%)	SO_3 content (%)
		3 d	28 d	3 d	28 d				
70 min	6 h	20	38.5	3.6	7.8	3.4	3.6	2.3	2.8

Table 2: Cement mortar mixture scheme.

Number of specimens	Water cement ratio, w/c	Cement (kg/m^3)	Water (kg/m^3)	River sand (kg/m^3)
3	0.45	360	162	760

(a) (b)

Figure 1: Main experimental equipment. (a) NMR test system. (b) Freeze-thaw cycle test machine.

Figure 2: Cement mortar specimens.

Freeze-thaw causes the surface of cement mortar to change and fall off, and the quality change of cement mortar can be used as the evaluation index of the damage degree of the cement mortar specimen during the freeze-thaw cycle: the greater the mass loss, the greater the damage to cement mortar caused by the freeze-thaw cycle. Table 3 shows the quality of cement mortar after different freeze-thaw cycles. It shows that, as the number of freeze-thaw cycles increases, the quality of cement mortar is decreasing gradually, and it was reduced by about 8% after 100 freeze-thaw cycles.

Table 4 shows the changes law of mechanical parameters during the freeze-thaw cycle, and it shows that, as the number of freeze-thaw cycles increased, the compressive strength, tensile strength, and elastic modulus of cement mortar specimens have decreased.

4. NMR Characteristics of Cement Mortar during Freeze-Thaw Cycles

4.1. NMR T_2 Spectrum Distribution. The changes of an NMR T_2 spectrum could reflect the structural changes of pores within cement mortar. The sizes of pores in cement mortar specimens are in proportion to the fluid traverse relaxation time T_2. When T_2 is small, it means that the sizes of pores in cement mortar specimens are small; the location of peaks in the T_2 spectrum is directly related to the size of pores, and the peak value in the T_2 spectrum reflects the concentration degree of the distribution of pore sizes within cement mortar specimens. Therefore, the changes of T_2 spectrum could qualitatively describe the structural changes of pores inside the cement mortar specimens. Figure 4 shows the T_2 distribution of the cement mortar specimens after 25, 50, 75, and 100 freeze-thaw cycles.

It can be seen that the T_2 spectrum distribution is mainly presented by 3 peak images: the first peak area is the largest, located near at 1.5 ms; the second one is smaller than the first one, located near at 75 ms; and the third peak is almost invisible, located near at 750 ms. The first spectrum peak in the T_2 spectrum curve was considered as small pores, and the second and third spectrum peak were large pores. This indicates that the internal pores of cement mortar are mainly small pores, and the proportion of large pores and large pores is low. During the process of 100 freeze-thaw cycles, the T_2 spectrum peak of cement mortar gradually increased, and the curve gradually expanded outward, which shows

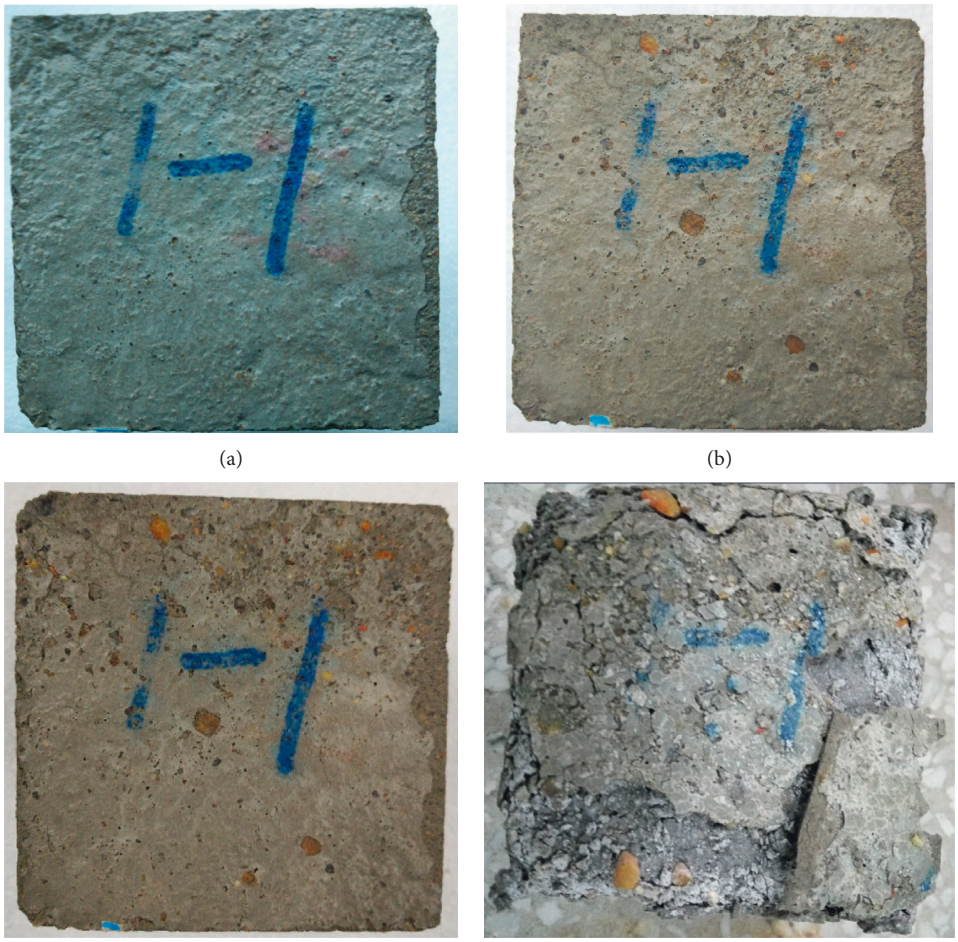

(a) (b) (c) (d)

Figure 3: Surface changes during freeze-thaw cycles. (a) 25 cycles. (b) 50 cycles. (c) 75 cycles. (d) 100 cycles.

Table 3: Masses of cement mortar after different freeze-thaw cycles (g).

Groups	Cycles				
	0	25	50	75	100
A1	715.7	713.9	709.1	703.7	663.9
A2	714.6	712.3	707.2	702.5	658.4
A3	715.8	713.9	710.1	705.5	667.3
Average	715.4	713.4	708.8	703.9	663.2

Table 4: Mechanical parameters of cement mortar during freeze-thaw cycles (MPa).

Mechanical parameters	Cycles				
	0	25	50	75	100
Compressive strength (MPa)	21.385	18.448	18.874	17.875	9.262
Tensile strength (MPa)	2.182	1.789	1.578	1.327	0.346
Elastic modulus (GPa)	0.692	0.803	0.735	0.668	0.270

there are more internal pores produced inside the cement mortar after freeze-thaw cycles, and the small pores gradually become larger pores.

4.2. T_2 Spectra Area Variation. Table 5 shows the variation of T_2 spectrum area of cement mortar specimens after 100 freeze-thaw cycles. It can be seen that the total spectrum area increased with the increasing of freeze-thaw cycles. The proportion of the first spectrum peak area is more than 90%, which means the internal pores of cement mortar are mainly small pores. However, as there is an increase in the number of freeze-thaw cycles, the proportion of the second peak and the third peak is gradually increasing, while the first peak is decreasing, as shown in the ratio change rule of each spectrum peak in the T_2 spectrum in Figure 5, which shows that the small pores inside the cement mortar are gradually getting larger, and the number of larger pores are increasing. Meanwhile, there are some new micropores constantly appearing, this change objectively reflects the microcosmic change and destruction mechanism of cement mortar during freeze-thaw cycles.

4.3. Relationship between NMR Characteristics and Its Mechanical Properties. The variation curves of compressive strength, splitting tensile strength, and magnetic resonance porosity of cement mortar during freeze-thaw cycles were shown in Figure 6; it can be seen that the

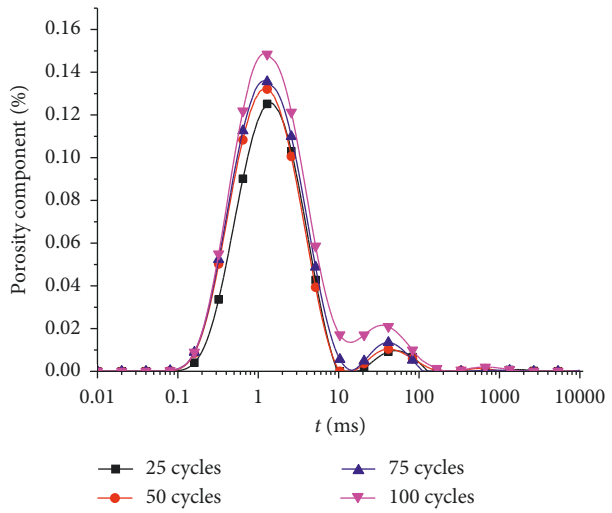

Figure 4: NMR T_2 spectrum distribution during freeze-thaw cycles.

Table 5: Spectrum area of cement mortar specimens during freeze-thaw cycles.

Cycles	Total spectrum area	Proportion of the first spectral peak area (%)	Proportion of the second spectral peak area (%)	Proportion of the third spectral peak area (%)
25	4172	95.72404	4.068485	0.200453
50	4625	95.31089	4.352558	0.328246
75	4982	95.19268	4.612204	0.172329
100	5847	90.6981	8.721188	0.573623

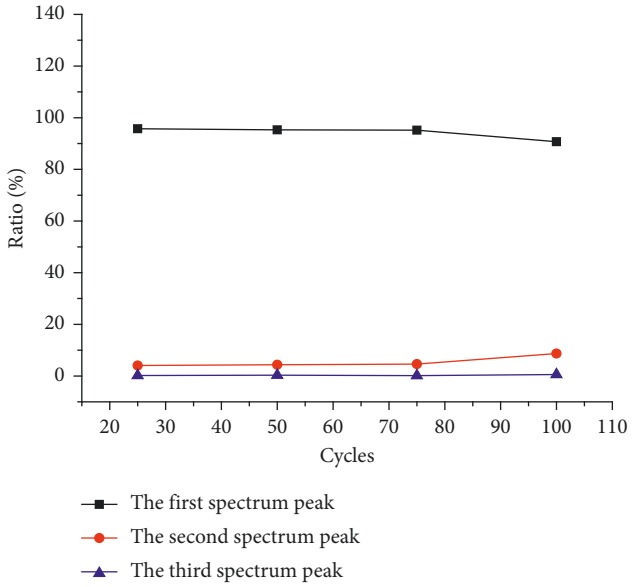

Figure 5: Ratio change rule of each spectrum peak in the T_2 spectrum.

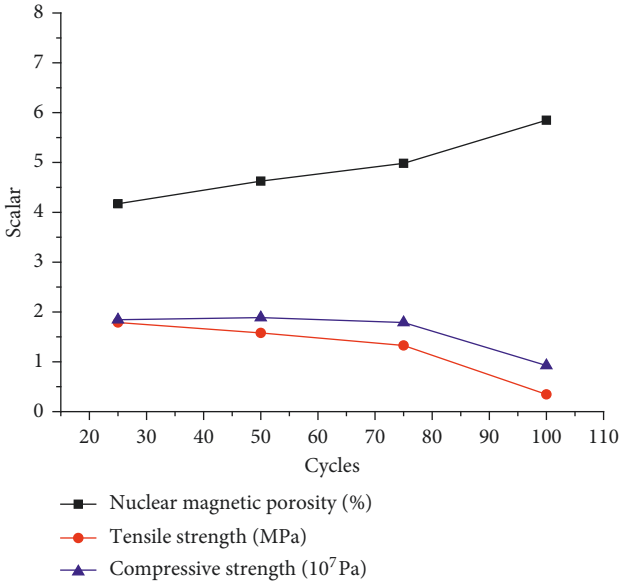

Figure 6: NMR characteristics and mechanical properties of cement mortar during freeze-thaw cycles.

nuclear magnetic porosity increased during freeze-thaw cycles, and there is a tendency to accelerate. While the tensile strength and compressive strength of the cement mortar decreased, the rate of decline is accelerating. It shows the porosity of cement mortar is negatively correlated with its tensile strength and compressive strength. The internal porosity of the cement mortar has been expanded after freezing, and its mechanical properties are gradually decreasing.

5. Conclusion

(1) When the cement layered while pouring module during freeze-thaw cycles, there was a weak side on the surface that damaged after many freeze-thaw cycles. As freeze-thaw cycles increased, the quality of cement mortar gradually decreased and the compressive strength, crack tensile strength, and elastic modulus of cement mortar also decreased.

(2) The NMR technology had been applied to study the microstructure of cement mortar during the freeze-thaw cycle for the first time. The magnetic resonance T_2 spectrum of cement mortar has three peaks, and the first crest ratio is over 90%, indicating that the internal pores of cement mortar are mainly microporous. With the increasing of freeze-thaw cycles, the microporosity inside cement mortar is gradually enlarged and new pores are constantly produced.

Data Availability

The data used to support the findings of this study are available from the corresponding author upon request.

Conflicts of Interest

The authors declare that there are no conflicts of interest regarding the publication of this paper.

Authors' Contributions

Taoying Liu carried out the figure preparation, analysis, manuscript preparation, and editing. Yunmin Wang and Keping Zhou planned and designed the research. Feng Gao contributed the conduct. Shenghua Xie performed the data collection.

Acknowledgments

This paper was funded by the National Key Research and Development Program of China (2018YFC0808404); the Key Research & Development Program of Hunan Province (2017GK2190); China Postdoctoral Science Foundation funded project (2018M643003); Anhui Postdoctoral Foundation Fund Project (2017B201); project was (2018JJ3676) supported by the Natural Science Foundation of Hunan Province; and open fund was provided by the State Key Laboratory of Safety and Health for Metal Mine (2016-JSKSSYS-02, 2018-JSKSSYS-02, and 2018-JSKSSYS-04). And we would like to express our thanks to Wenwu Tan for his help in this paper.

References

[1] R.-H. Cao, P. Cao, H. Lin, G. Ma, and Y. Chen, "Failure characteristics of intermittent fissures under a compressive-shear test: experimental and numerical analyses," *Theoretical and Applied Fracture Mechanics*, vol. 96, pp. 740–757, 2018.

[2] Y. Tian, *Study on Early Strength of Additive Cement Mortar and Nuclear Magnetic Resonance Characteristics under Freeze-Thaw*, Central South University, Changsha, China, 2015.

[3] H. Lin, W. Xiong, and Q. Yan, "Modified formula for the tensile strength as obtained by the flattened Brazilian disk test," *Rock Mechanics and Rock Engineering*, vol. 49, no. 4, pp. 1579–1586, 2015.

[4] Y. Zhao, L. Zhang, W. Wang, J. Tang, H. Lin, and W. Wan, "Transient pulse test and morphological analysis of single rock fractures," *International Journal of Rock Mechanics and Mining Sciences*, vol. 91, pp. 139–154, 2017.

[5] C. J. Korhonen, "Antifreeze admixtures for cold regions concreting a literature review," Special Report 90–32, U.S. Army Corps of Engineers Cold Regions Research & Engineering Laboratory, Hanover, NH, USA, 1990.

[6] J. Meng, P. Cao, J. Huang, H. Lin, Y. Chen, and R. Cao, "Second-order cone programming formulation of discontinuous deformation analysis," *International Journal for Numerical Methods in Engineering*, 2019, In press.

[7] H. Lin, H. Wang, X. Fan, P. Cao, and K. Zhou, "Particle size distribution effects on deformation properties of graded aggregate base under cyclic loading," *European Journal of Environmental and Civil Engineering*, vol. 2018, pp. 1–18, 2018.

[8] R. Polat, "The effect of antifreeze additives on fresh concrete subjected to freezing and thawing cycles," *Cold Regions Science and Technology*, vol. 127, pp. 10–17, 2016.

[9] T. C. Powers, "The air requirement of frost resistant concrete," in *Proceedings of the Highway Research Board*, vol. 29, pp. 184–211, Washington, DC, USA, December 1949.

[10] Y. Chen and H. Lin, "Consistency analysis of Hoek-Brown and equivalent Mohr-coulomb parameters in calculating slope safety factor," *Bulletin of Engineering Geology and the Environment*, vol. 2018, pp. 1–13, 2018.

[11] R. Polat, R. Demirboğa, M. B. Karakoç, and İ. Türkmen, "The influence of lightweight aggregate on the physico-mechanical properties of concrete exposed to freeze-thaw cycles," *Cold Regions Science and Technology*, vol. 60, no. 1, pp. 51–56, 2010.

[12] A. Türkmen, O. Zlatkovski, and V. Sopov, "Regularities of ıce formation and estimation of frost attack danger. Frost resistance of concrete," in *Proceedings of the International Workshop on Frost Resistance of Concrete*, pp. 213–221, Madrid, Spain, September 2002.

[13] W. Yixian, G. Panpan, D. Feng, L. Xian, Z. Yanlin, and L. Yan, "Behavior and modeling of fiber-reinforced clay under triaxial compression by combining the superposition method with the energy-based homogenization technique," *International Journal of Geomechanics*, vol. 18, no. 12, article 04018172, 2018.

[14] L. Jia, M. Chen, L. Sun et al., "Experimental study on propagation of hydraulic fracture in volcanic rocks using industrial CT technology," *Petroleum Exploration and Development*, vol. 40, no. 3, pp. 405–408, 2013.

[15] Y. Wang, S. Wang, Y. Zhao, X. Li, P. Guo, and Y. Liu, "Analysis of fracturing characteristics of unconfined rock plate under edge on impact loading," *European Journal of Environmental and Civil Engineering*, 2019, In press.

[16] J. Zuo, X. Wei, J. Pei, and X. Zhao, "Investigation of meso-failure behaviors of Jinping marble using SEM with bending loading system," *Journal of Rock Mechanics and Geotechnical Engineering*, vol. 7, no. 5, pp. 593–599, 2015.

[17] L. Zhao, Z. Fang, C. Qi, B. Zhang, L. Guo, and K. I.-I. L. Song, "Numerical study on the pipe flow characteristics of the cemented paste backfill slurry considering hydration effects," *Powder Technology*, vol. 343, pp. 454–464, 2019.

[18] X. Fan, K. Li, H. Lai, Y. Xie, R. Cao, and J. Zheng, "Internal stress distribution and cracking around flaws and openings of rock block under uniaxial compression: a particle mechanics approach," *Computers and Geotechnics*, vol. 102, no. 10, pp. 28–38, 2018.

[19] X.-D. Zhao, H.-X. Zhang, and W.-C. Zhu, "Fracture evolution around pre-existing cylindrical cavities in brittle rocks under uniaxial compression," *Transactions of Nonferrous Metals Society of China*, vol. 24, no. 3, pp. 806–815, 2014.

[20] W. Ding, Y. Wu, Y. Pu et al., "History and present situation of X-ray computerized tomography (CT) of rocks," *Seismology and Geology*, vol. 25, no. 3, pp. 467–476, 2013.

[21] X. Fan, R. Chen, H. Lin, H. Lai, C. Zhang, and Q. Zhao, "Cracking and failure in rock specimen containing combined flaw and hole under uniaxial compression," *Advances in Civil Engineering*, vol. 2018, Article ID 9818250, 15 pages, 2018.

[22] K. Zhou, T. Liu, and Z. Hu, "Exploration of damage evolution in marble due to lateral unloading using nuclear magnetic resonance," *Engineering Geology*, vol. 244, pp. 75–85, 2018.

[23] P. Cao, T. Liu, C. Pu, and H. Lin, "Crack propagation and coalescence of brittle rock-like specimens with pre-existing cracks in compression," *Engineering geology*, vol. 187, pp. 113–121, 2015.

[24] G. Coates, L. Xiao, and M. Prammer, *NMR Logging Principles and Application*, Petroleum Industry Press, Beijing, China, 2007.

[25] D. Matias, J. de Brito, A. Rosa, and D. Pedro, "Mechanical properties of concrete produced with recycled coarse aggregates—influence of the use of superplasticizers," *Construction and Building Materials*, vol. 44, pp. 101–109, 2013.

[26] M. E. Ramia and C. A. Martín, "Sedimentary rock porosity studied by electromagnetic techniques: nuclear magnetic resonance and dielectric permittivity," *Applied Physics A*, vol. 118, no. 2, pp. 769–777, 2014.